SANDIP KUMAR, ASISH MALAS, CHAPAL KUMAR DAS[*)]

Indian Institute of Technology
Materials Science Centre
Kharagpur, India-721302

Layered double hydroxide modified with linseed compounds for polyurethane elastomer nanocomposites

Summary — Layered double hydroxides (LDHs) are a class of layered inorganic materials, containing basic layers of metal hydroxides. Between these layers anions and water molecules are accommodated. Interlayer anion can be replaced by wide range of organic and inorganic anions and this key feature of LDH opens new fields of applications. In this study magnesium and aluminum based LDH was modified with linseed compounds *using the* regeneration method. Modified LDH samples were characterized by X-ray diffraction (XRD), Fourier transform infrared spectroscopy (FT-IR), high resolution transmission electron microscopy (HR-TEM), scanning electron microscopy (SEM) and field emission scanning electron microscopy (FE-SEM). XRD results indicate that anionic spacer has gone inside the gallery space, which is evident from increased interlayer spacing. FT-IR study suggests the presence of spacer moiety in modified LDH. From FE-SEM study, it was observed that the shape and texture of LDH platelets have changed (they were hexagonal and smooth before modification). Unmodified and modified LDH were applied to prepare polyurethane nanocomposites (PUR/LDH and PUR/LLDH, respectively). Nanocomposite PUR/LLDH was characterized by better mechanical and thermal properties in comparison with PUR/LDH and neat polyurethane.
**Keywords**: layered double hydroxide, regeneration method, nanocomposite, linseed compounds, polyurethane.

WARSTWOWY PODWÓJNY WODOROTLENEK MODYFIKOWANY ZWIĄZKAMI Z SIEMIENIA LNIANEGO DO OTRZYMYWANIA ELASTOMEROWYCH NANOKOMPOZYTÓW POLIURETANOWYCH
Streszczenie — Warstwowe podwójne wodorotlenki (LDH) są klasą warstwowych materiałów nieorganicznych, składających się z podstawowych warstw wodorotlenków metali i umieszczonej pomiędzy nimi warstwy anionów i cząsteczek wody. Aniony warstwy pośredniej mogą być zastąpione przez szereg anionów organicznych i nieorganicznych, co otwiera nowe pola zastosowań modyfikowanych LDH. W ramach tej pracy LDH magnezu i glinu modyfikowano metodą regeneracji związkami z siemienia lnianego. Próbki zmodyfikowanego LDH (oznaczane LLDH) charakteryzowano metodami dyfrakcji rentgenowskiej (XRD), spektroskopii w podczerwieni z transformacją Fouriera (FT-IR), transmisyjnej mikroskopii elektronowej wysokiej rozdzielczości (HR-TEM), skaningowej mikroskopii elektronowej (SEM) i skaningowej mikroskopii elektronowej z emisją polową (FE-SEM). Wyniki badań próbek LLDH metodą XRD wykazały, że warstwa anionowa umieściła się wewnątrz przestrzeni pomiędzy warstwami kationów, o czym świadczyły zwiększone odstępy międzywarstwowe. Badania FT-IR tych próbek dowiodły obecności ugrupowań charakterystycznych dla wprowadzonych na skutek modyfikacji anionów. Rezultaty badań FE-SEM pokazały że kształt i tekstura płytek LDH zmienia się z heksagonalnych i gładkich przed modyfikacją na bardziej nieregularne. Niemodyfikowany i modyfikowany LDH zastosowano do otrzymania nanokompozytów poliuretanowych (odpowiednio PUR/LDH i PUR/LLDH). Nanokompozyty PUR/LLDH charakteryzowały się lepszymi właściwościami mechanicznymi i termicznymi niż PUR/LDH i czysty poliuretan.
Słowa kluczowe: warstwowy podwójny wodorotlenek, metoda regeneracji, nanokompozyt, związki siemienia lnianego, poliuretan.

Layered double hydroxides (LDHs) are one of the nano-ordered layered compounds. LDHs, also known as anionic clays, are a family of compounds which deserve much attention in recent years [1—3]. Most of the LDHs' structure corresponds to that of hydrotalcite, a natural magnesium aluminum hydroxycarbonate. The general formula of LDH is

$$\left[M^{II}_{1-X} M^{III}_{X} (OH)_2 \right]^{X+} \left(A^{N-} \right)_{X/N} \cdot Y\, H_2O.$$
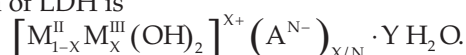
[*)] Corresponding author; e-mail: chapal12@yahoo.co.in

Where, M^{II} is a divalent metal such as Ca^{2+}, Mg^{2+}, Zn^{2+} *etc.*, M^{III} is a trivalent metal such as Al^{3+}, Co^{3+}, Cr^{3+} *etc.* and A^{N-} is an anion such as Cl^-, CO_3^{2-}, NO_3^- *etc.* X is given by $M^{III}/M^{II} + M^{III}$, X value varies from 0.25 to 0.33 [4]. The structure of LDHs can be best explained analogous to mineral Brucite $[Mg(OH)_2]$. Brucite consists of a hexagonal close packing of hydroxyl ions with alternate octahedral sites occupied by divalent ions. In LDHs some of the divalent cations of these Brucite-like sheets are isomorphously substituted by a trivalent cation. The occupancy of a trivalent ion generates a net positive charge on the mixed metal hydroxide layer and anions are present in the interlayer space to compensate this positive charge. In natural hydrotalcite these interlayer anions are normally carbonate and water molecules also exist in the interlayer space, associated to the anions. On the other hand, the electric charge of the layers and the interlayer ions is just the opposite of that found in silicate clays (cationic clays). For all these reasons, these materials are usually known as layered double hydroxides, anionic clays or hydrotalcite. As in anionic clays, the interlayer anions are easily exchanged by various inorganic and organic anions, as for example carbonate ion has been exchanged by many different anions [5—7]. Replacing capability of an interlayer ion has a broad field of applications such as catalysts or catalyst supports, processing of selective chemical nanoreactors, separation and membrane technology, filtration, scavenging and controlled release of anions, electroactive photoactive materials, nanofillers *etc.* [2, 8—11].

Use of LDHs in polymer nanocomposites is recently investigated. LDHs as a nanofiller improves various technical properties (such as mechanical, thermal and barrier) of polymer matrices. But because of high charge density [12—15] and low interlayer spacing its dispersion in polymer is a challenging problem. It can be solved by replacing the interlayer anion by a long chain anionic spacer. A wide range of methods such as anion exchange, regeneration, co-precipitation and thermal reaction can be used for modification of LDHs. Selectivity of these processes depends on the starting precursor.

In the present work magnesium-aluminum hydroxycarbonate (Hycite 713) was first modified by linseed compounds *using the* regeneration route [16] and then polyurethane (PUR) and LDH elastomeric nanocomposites were prepared.

EXPERIMENTAL

Materials

In this study Mg and Al based LDH containing carbonate as interlayer anion (Hycite 713) was used. It was supplied by Süd-Chemie AG (Germany).

Linseed oil used was supplied by Kemphasol Mumbai (India). Table 1 shows the composition of linseed oil. Sodium salt of these compounds was made to achieve better

solubility in water by treating the supplied material with sodium hydroxide, the procedure was discussed elsewhere [17].

T a b l e 1. Composition of linseed oil

Typical fatty acid	Content, wt. %
Palmitic acid	6.0
Stearic acid	2.5
Arachidic acid	0.5
Oleic acid	19.0
Linoleic acid	24.1
Alpha linolenic acid	47.4
Others	0.5

Polyurethane (PUR, Urepan 600) used in this study was supplied by Rhein Chemie (Germany). It is toluene diisocyanate and polyester based elastomer.

Standard isocyanate curative (2,4-toluene diisocyanate) used in this study was supplied by Rhein Chemie (Germany).

Modification of LDH

Commercially available LDH (Hycite 713) was modified by regeneration method [18]. First Hycite 713 was calcined in a muffle furnace at 600 °C for three hours which results in layered metal oxide or more precisely we can say in solid solution of magnesium and aluminum oxides. Afterwards it was cooled down to 30 °C. Next LDH was heated at heating rate 5 °C/min. Fast heating causes destruction of the layered structure due to the expulsion of carbon dioxide and water. This calcined LDH was added to aqueous solution of sodium salt of linseed compound under vigorous stirring for 72 hours. During the modifications process temperature was kept constant at 70 °C to maintain the solubility of the linseed compound in water. Modified LDH was separated from the solution by filtration and then it was washed three times with hot water and dried at 60 °C for 4 hours in an oven. Modified LDH was linseed oil modified layered double hydroxide (LLDH).

Preparation of LDH and PUR nanocomposites

Nanocomposites were prepared by solution intercalation followed by mechanical mixing (the nanocomposites terminology was used because by definition if the filler is having any one dimension in nanometer range then the composite is termed as nanocomposite). First, 3 g of polyurethane were dissolved in 250 cm^3 of tetrahydrofuran. 1 g of LLDH was added slowly to the above solution under vigorous stirring. Then the complete system was kept under constant stirring for 4 h. Finally the solvent was evaporated and resulting solution-casted composite was

mixed with 30 g of PUR in haake-type internal mixer with a rotor speed of 30 rpm at room temperature. The amount of polyurethane and filler in the nanocomposite was 33 g and 1 g, respectively (the filler percentage in the composition was about 3 wt. %). In the last step of mixing a suitable amount of curative (about 10 wt. % of 2,4-toluene diisocyanate) was added. Finally, elastomeric composites were vulcanized under pressure of 10 MPa at 170 °C. The nanocomposite was polyurethane/linseed oil modified layered double hydroxide nanocomposites (PUR/LLDH).

Methods of testing

X-ray diffraction (XRD) measurements were carried out on Rigaku Miniflex diffractometer using copper target (Cu-Kα) at the scanning rate of 20 °/min from 2 to 15° (chart speed of 10 mm/2θ, range of 5000 cycle/s and a slit of 0.2 mm), operating at the voltage of 40 kV and current 20 mA. Interlayer spacing was calculated using Bragg's equation.

The dispersion morphology of composites was observed in high resolution transmission electron microscope (HR-TEM, JEOL 2100). For the HR-TEM image observation, ultra thin cross-section of specimens was cut out by using Leica Ultra cut UCT ultramicrotome.

Thermogravimetric analysis (TGA) was carried out using a Dupont TGA-2100 thermal analyzer in the temperature range from 50 to 600 °C, at the heating rate of 10 °C/min under the nitrogen atmosphere.

FT-IR analysis was performed in the range from 650 cm^{-1} to 4000 cm^{-1} using Thermonicolet/Nexus 870 FT-IR spectrometer. The powdered samples were mixed with KBr in a 1:200 mass ratio and pressed in the form of pellets for measurement. For measurements the polymeric composite thin films of thickness in the range 100—250 μm were compression molded.

Mechanical properties were determined with universal tensile testing machine (Hounsfield H 10KS) under ambient conditions: at 25 ± 2 °C and relative humidity of 75 %. For each set 5 samples were tested and the result presented were the average values. The samples were

prepared according to ASTM D 638 standard. The moduli at 100 % and 300 % elongation, tensile strength and elongation at break (in %) were measured at room temperature. The initial length of the specimen was 25 mm and the speed of jaw separation was 500 mm/min.

Scanning electron microscopy (SEM) study was carried out in VEGA TESCAN//LSU. The tensile-fractured samples were coated with a thin layer of gold. During scanning vacuum should be in the order of 10^{-4} to 10^{-6} mm Hg (0.013—0.00013 Pa).

Field emission scanning electron microscopy (FE-SEM) analysis was performed using a Carl Zeiss-SUPRATM 40. The fillers are coated with a thin layer of gold (approximately 5 nm). During the scanning of the samples the vacuum was in the order of 10^{-4}—10^{-6} mm Hg.

RESULTS AND DISCUSSION

Thermogravimetric analysis

The thermal analysis of the LDH is primarily aimed to investigate the decomposition behavior of the organic fraction and also the metal hydroxide layers. This was carried out by identifying various decomposition stages and the corresponding temperature range in the TGA curves. The comparison of the TGA curves of the LLDH with that of the unmodified one gives an indication how the interlayer anionic moiety influence the decomposition of the host material. TGA and corresponding differential curve (DTGA) of unmodified LDH and LLDH are shown in Figure 1. The unmodified LDH shows two-stage decomposition process: a low temperature (up to about 225 °C) dehydration stage due to the loss of interlayer water and a high temperature decomposition (225—500 °C) stage due to the loss of interlayer carbonate and dehydroxylation of the metal hydroxide layers.

Modification of the LDH with linseed compounds significantly changes its thermal decomposition behavior in comparison to the unmodified LDH, especially at the second stage of the decomposition process, which results in complete collapse of materials structure.
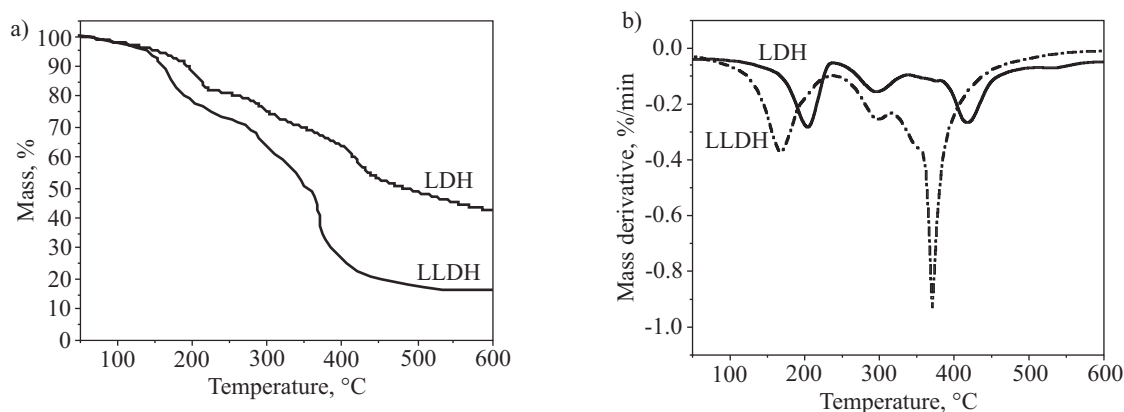

Fig. 1. The results of thermogravimetric analysis for LDH (curve 1) and LLDH (curve 2): a) TGA, b) DTGA
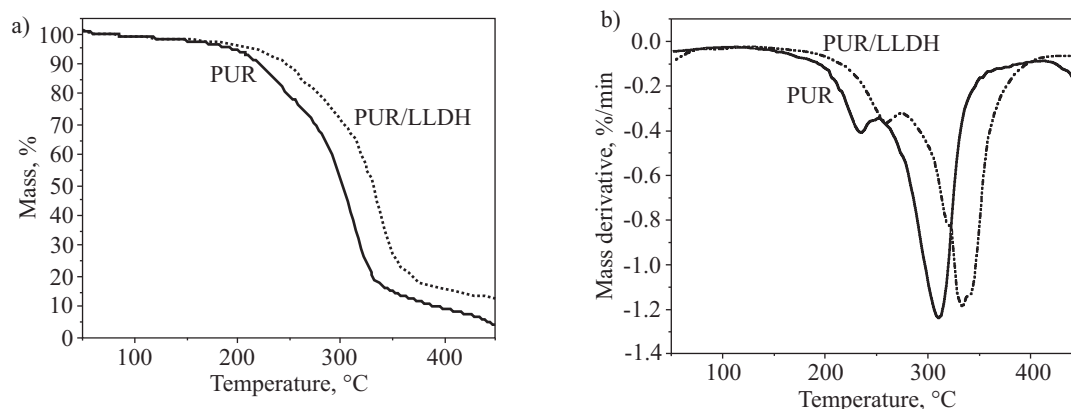
Fig. 2. The results of thermogravimetric analysis for PUR (curve 1) and PUR/LLDH (curve 2): a) TGA, b) DTGA

The loss of interlayer water molecules up to temperature about 225 °C in the sample LLDH is greater in comparison to unmodified LDH, this indicates that in LLDH more water molecules are accommodated in the interlayer region, it may be because intercalation of anions of different fatty acid creates some free space between the double hydroxide layers. The second decomposition stage is also changed significantly after organic modification. The major weight loss in case of LLDH is caused by the decomposition of the interlayer anionic moiety. However, major dehydroxylation process of the host materials starts at around 300 °C.

TGA and DTGA curves of the pure PUR and PUR/LLDH nanocomposite is shown in Figure 2. Thermal degradation of PUR is mainly due to depolymerization which begins from 190 to 250 °C, due to the failure of urethane links, releasing the polyester and isocyanate (monomers) used to synthesize PUR chains. The monomers slowly volatilize during the continuous heating process. The complete volatilization of the resulting chain fragment is avoided by the dimerization of isocyanate to carbodiimides, which react with the alcohol groups to give relatively stable substituted urea. The decomposition in the third step occurs in the range from 300 to 400 °C, is related to the decomposition of urea groups and corresponds to the high temperature degradation of these stabilized structures to yield small quantity of carbonaceous char. Presence of LLDH causes distinct changes in the thermal decomposition behavior in comparison to unfilled polyurethane. With the addition of only 3 wt. % of LLDH, the first decomposition stage in unfilled polyurethane is not only shifted to a higher temperature range but also the extent of mass loss during this stage decreases.

XRD analysis

XRD results of unmodified LDH, LLDH and PUR/LLDH composite from 2 to 14° range are shown in Figure 3. As expected, the position of the first order basal diffraction < 003 > for LLDH is shifted to a lower 2θ value indicating intercalation of anionic moiety in gallery space. The LLDH sample show distinct diffraction peak corresponding to $d = 0.78$ nm due to some remained unmodified LDH, because the modification was performed in the presence of air. Intensity of peak LLDHs plot also decreases which indicates that the modification leads to
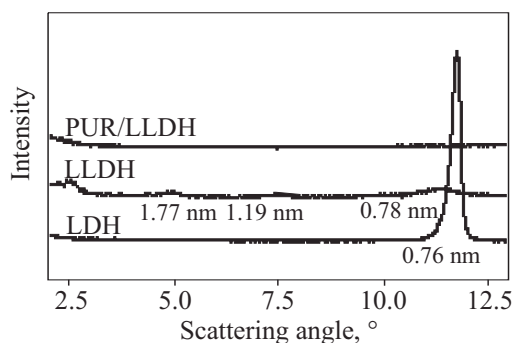

Fig. 3. XRD plots of LDH (curve 1), LLDH (curve 2), and PUR/LLDH (curve 3)

low crystalline LDH. In the case of LLDH three peaks occur because linseed compound is a mixture of different fatty acids. In the case of PUR/LLDH nanocomposite containing about 3 wt. % of LLDH no peak has been observed. This observation suggests that the organically modified LDH layers are delaminated or completely exfoliated in the PUR matrix. Similar results have been reported by Acharya *et al.* [19], where they ascribed the disappearance of the XRD peaks corresponding to LDH, in the EPDM/LDH nanocomposites to the partial exfoliated structure of LDH. Hence, in our case also the partial exfoliation can be confirmed by XRD plots and which can be substantiated from the TEM images.

XRD provides a partial picture of the distribution of nanofiller and absence of peak corresponding to d-spacing does not always indicate the delamination of filler in polymer matrix, because XRD is unable to detect regular stacking exceeding 8.8 nm [20]. Therefore, to study the morphology of the nanocomposites it is required microscopic investigation [19].

HR-TEM study

Figure 4 shows the HR-TEM images of PUR/LLDH and PUR/LDH nanocomposites with 3 wt. % of LDHs. The dark lines represent the LDH layers, whereas the bright area represents PUR matrix. It is also evident from
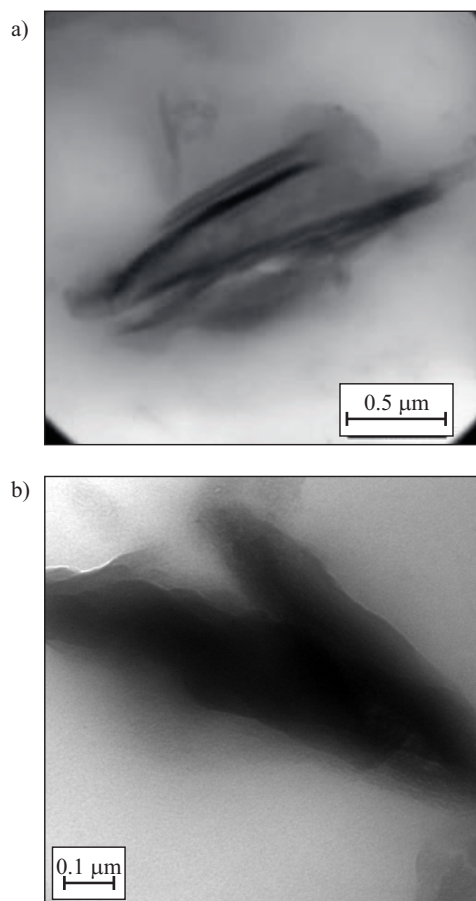

Fig. 4. HR-TEM image of: a) PUR/LLDH, b) PUR/LDH

the HR-TEM image that the LLDH layers are delaminated in polyurethane matrix. Although the HR-TEM pictures have been taken in a small area they have confirmed the delamination over the large area of the sample. These are the representative examples of one small section and it is quite clear from the images that there are delimitation of the LDH layers after the modification. It can be interpreted that the delamination is predominant but we cannot say that this is the complete exfoliation. Again the HR-TEM pictures clearly show that the delaminated section may be include several layers suggesting single layer delamination. Extremely exfoliated structure is not achieved. Maybe we need different types of modifications, in order to achieve the complete exfoliation of LDH in the PUR matrix. In the case of PUR/LDH nanocomposite layers are agglomerated. HR-TEM study also indicates the improvement in mechanical properties. Better dispersion results in better mechanical properties.

FT-IR analysis

The FT-IR spectra of the unmodified and modified LDH are shown in Figure 5. LLDH spectrum shows two types of bands: one corresponding to the anionic species intercalated between the host LDHs layers and the other
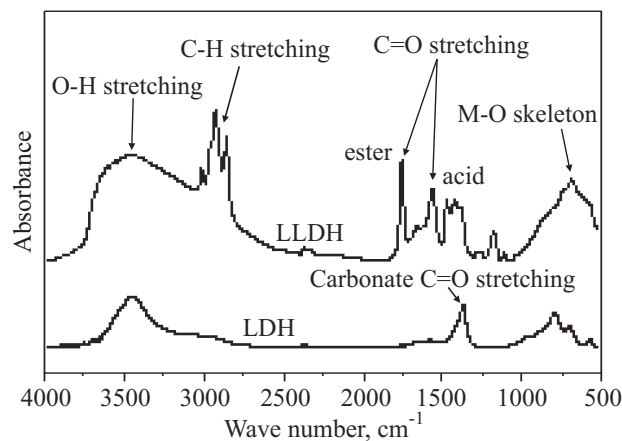

Fig. 5. FT-IR spectra of LDH (curve 1) and LLDH (curve 2)

corresponding to host LDH materials. This has been shown in detail in Figure 5 and Table 2. LLDH sample shows strong absorption bands in the range of 2850—2965 cm^{-1} corresponding to the -CH_2- stretching vibration of the hydrocarbon tail present in each of the surfactant anions. The peak appears at 1560 cm^{-1} corresponds to carboxylic C=O stretching present in sodium salt of linseed oil and the peak at 1765 cm^{-1} corresponds to ester C=O stretching. The band around 650 cm^{-1} originates from the lattice vibration of the hydroxide sheet and the broad band in the range 3200—3700 cm^{-1} is mainly from the O-H groups present in metal hydroxide layers and water molecules in the interlayer space. The appearance of characteristic vibration bands for CO_3^{2-} means there still exits some CO_3^{2-} in the interlayer region.
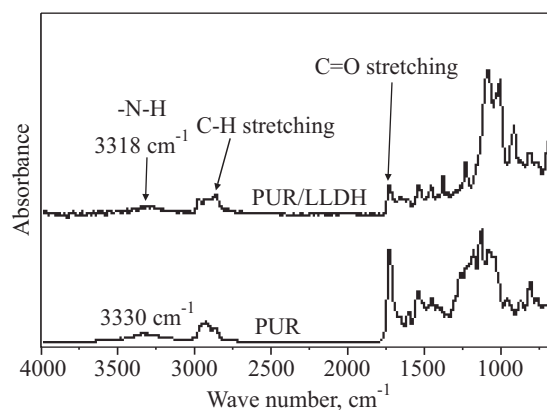

Fig. 6. FT-IR spectra of PUR (curve 1) and PUR/LLDH (curve 2)

T a b l e 2. **Characteristic bands observed on FT-IR spectra of LDH, LLDH, PUR and PUR/LLDH**

Material	Band frequency cm^{-1}	Types of vibrations
LDH	3420—3470	-OH stretching
	1356	CO_3^{2-}, C-O stretching
	550—750	M-O stretching
LLDH	2849—3015	C-H stretching
	1760	ester C=O stretching
	1551	asymmetric -COO- stretching
PUR	3330	urethane N-H stretching
	1728	urethane C=O stretching
PUR/LLDH	3318	urethane N-H stretching
	1715	urethane C=O stretching

FT-IR spectra of pure PUR and PUR/LLDH nanocomposites are shown in Figure 6. In case of nanocomposite apart from LDHs peaks, peaks around 1715 and 3318 cm^{-1} are the basic characteristics of C=O double bond and N-H bond of polyurethane. This confirms the presence of LLDH in PUR matrix.

Mechanical properties study

The effect of unmodified and modified LDH on the mechanical properties of PUR nanocomposites has been studied and the results are summarized in Table 3. Incorporation of LDH improves the mechanical properties of polyurethane elastomer. The enhancement in tensile modulus may be ascribed to the resistance put up by LDH itself, as well as the orientation and high aspect ratio of the LDH platelets. It is seen from Table 3 that the tensile strength and elongation at break for the nanocomposites containing unmodified and modified LDH are higher with respect to neat PUR. The tensile strength is increased by 20 and 40 % for PUR/LDH and PUR/LLDH, respectively. Similarly elongation at break is increased by 21 and 22.5 % for PUR nanocomposites containing LDH and LLDH, respectively. The increase in tensile strength is due to the strong interfacial interaction between the hydroxyl group of LDH and the polar urethane (-NHCOO) group of PUR through the hydrogen bond which is also confirmed by FT-IR. It also appears that the delaminated LDH layers transfer stress from LDH itself and directly enhance the stiffness of PUR nanocompo-

sites. The enhancement in elongation at break may be due to the entanglement of the polymer chain and the synergistic effect of chain slippage and orientation of LDH layers.

FE-SEM analysis of LDH

Magnesium and aluminum based LDH clays usually show platelets-like morphology. The size distribution of the particles depends mostly on the synthesis conditions and varies from few hundred nm to few micrometers in lateral dimensions. The FE-SEM images of unmodified and modified LDH are presented in Figure 7. The FE-SEM micrograph of the unmodified LDH (Fig. 7a) shows this particle geometry where the primary plate-like particles are characterized by distinct hexagonal
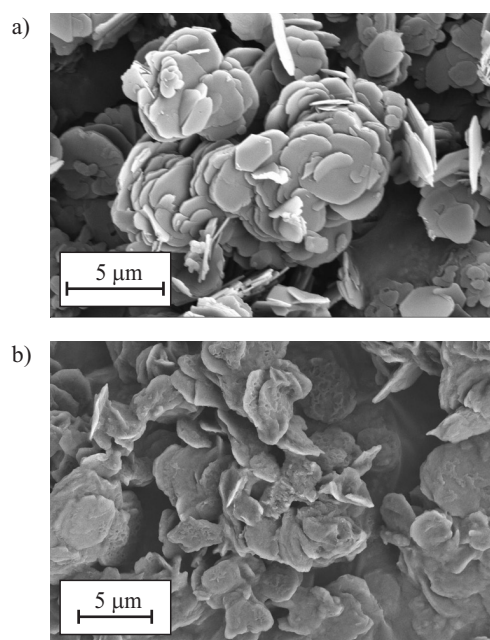

Fig. 7. FE-SEM images of: a) LDH, b) LLDH

shapes and sharp edges. The highly isometric nature of these primary particles is also apparent. The lateral dimension of these plate-like particles varies within few micrometers whereas the thickness hardly exceeds few hundred nm. The regeneration process restores the metal hydroxide sheets of the LDH. In the case of LLDH morphology (Fig. 7b) is more irregular and texture is also

T a b l e 3. **Mechanical properties of neat PUR and its nanocomposites**

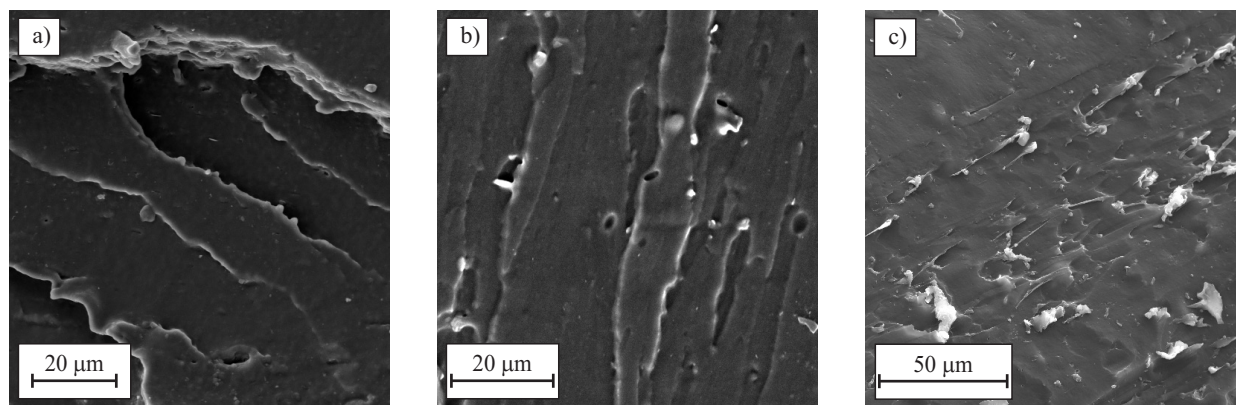| Sample	Tensile strength MPa	Elongation at break, %	Modulus at 100 % elongation, MPa	Modulus at 300 % elongation, MPa	Tear strength N/mm
PUR	7.50 ± 0.3	400 ± 20	3.05 ± 0.2	6.57 ± 0.5	27.70 ± 2.0
PUR/LDH	9.05 ± 0.2	485 ± 10	3.86 ± 0.3	7.61 ± 0.4	32.50 ± 3.0
PUR/LLDH	10.54 ± 0.3	490 ± 5	4.72 ± 0.3	8.12 ± 0.5	33.72 ± 1.5

Fig. 8. SEM images of: a) PUR, b) PUR/LDH, c) PUR/LLDH

different in comparison to unmodified LDH. This difference in texture may be due to the modification, not entirely due to the deposition of oil, as we have modified the LDH by the sodium salt of linseed oil as described in the earlier section. However the presence of minute amount of oil cannot be avoided.

SEM study of fractured surfaces

Fracture surface of the nanocomposites gives an idea about the mechanism of fracture and dispersion of fillers in the polymer matrix. Figure 8 displays SEM micrographs of the tensile fractured surfaces of neat PUR and its nanocomposites (PUR/LDH and PUR/LLDH) containing 3 wt. % of filler. The LDH filled PUR nanocomposites both unmodified and modified show rough fractured morphology in comparison to the pure one. The increase in roughness of the fractured surface may be due to the dispersion of LDH or LLDH in the PUR matrix. Among the PUR nanocomposites, PUR/LLDH shows a highly rough and tortuous path of fracture in comparison to PUR/LDH and pure PUR. The dispersion of LDHs platelets in the rubber alters the crack path along the direction depending on their orientation in the PUR matrix. Hence, it may form higher resistance to crack propagation that can lead to increase in tensile strength of the nanocomposites compared to the pure one.

CONCLUSION

In the present study magnesium and aluminum based LDH was successfully modified by linseed compounds. Then LLDH was dispersed in the PUR matrix by solution mixing followed by mechanical mixing and the effect of modification of LDH on the properties of PUR nanocomposites was studied. The XRD analysis of the LLDH corroborates the increased basal spacing. HR-TEM study shows that layers of LLDH are partially exfoliated and intercalated in the PUR matrix in comparison to the agglomerated structure of pure LDH. LLDH based nano-

composite shows better mechanical properties compared to unmodified LDH added nanocomposites due to better dispersion of LLDH in the PUR matrix.

REFERENCES

1. Ambrogi V., Fardella G., Grandolini G., Perioli L., Tiralti M. C.: *AAPS Pharm. Sci. Tech.* 2002, **3**, No. 3, 77.
2. „Layered Double Hydroxides: Present and Future" (Ed. Rives V.), Nova Science Publishers, New York 2001.
3. Kovanda F., Balek V., Dorničák V., Martinec P., Mašláň M., Bílková L., Koloušek D., Bountsewa I. M.: *J. Therm. Anal. Calorim*. 2003, **71**, 727.
4. Cavani F., Trifiro F., Vaccari A.: *Catal. Today* 1991, **11**, 173.
5. Gardner G., Pinnavaia T. J.: *Appl. Catal., A* 1998, **167**, 65.
6. Newman S. P., Jones W.: *New J. Chem.* 1998, **22**, 105.
7. Moujahid E. M., Besse J. P., Leroux F.: *J. Mater. Chem.* 2002, **12**, 3324.
8. Saber O., Tagaya H.: *Rev. Adv. Mater. Sci.* 2005, **10**, 59.
9. Lee W. F., Chen Y. C.: *J. Appl. Polym. Sci.* 2004, **94**, 692.
10. Shan D., Cosnier S., Mousty C.: *Anal. Chem.* 2003, **75**, 3872.
11. Lin Y., Wang J. D., Evans G., Li D.: *J. Phys. Chem. Solids* 2006, **67**, 998.
12. Meyn M., Beneke K., Legaly G.: *Inorg. Chem.* 1990, **29**, 5201.
13. Marangoni R., Mikowski A., Wypych F.: *J. Colloid Interface Sci.* 2010, **351**, 384.
14. Marangoni R., Ramos L. P., Wypych F.: *J. Colloid Interface Sci.* 2009, **330**, 303.
15. Wypych F., Satyanarayana K. G.: *J. Colloid Interface Sci.* 2005, **285**, 532.
16. Poli A. L., Batista T., Schmitt C. C., Gessner F., Neumann M. G.: *J. Colloid Interface Sci.* 2008, **325**, 386.
17. Tilley F. W., Schaffer J. M.: *J. Infect. Dis.* 1925, **37**, 359.
18. Costa F. R., Leuteritz A., Wagenknecht U., Heinrich G.: *Appl. Clay Sci.* 2008, **38**, 153.
19. Acharya H., Srivastava S. K., Bhowmik A. K.: *Compos. Sci. Technol.* 2007, **67**, 2807.
20. Kornnmann X., Lindberg H., Berglund L. A.: *Polymer* 2001, **42**, 1303.